SYNTHESIS OF POLYPYRROLE'S SUPPORT ADSORBED ON BENTONITE. APPLICATIONS IN WASTEWATER TREATMENT

Amina BEN BOUABDALLAH[a] and Nacer-Eddine DJELALI[b,*]

[a] Laboratory UR / BEP (Research Unit Materials, Processes and development environment)
M'hamed Bouguera university of Boumerdes, Algeria
[b] Laboratory Treatment and Formatting of the Polymers (L.T.M.F.P).
M'hamed Bouguera university of Boumerdes, Algeria

Composites of polypyrrole and bentonite (PPy-B) have been synthesized by in situ polymerization of pyrrole in the presence of bentonite. Characterization and thermal stability of the composite have been performed by infrared Fourier transform spectroscopy (FTIR), X-ray diffraction (XRD) and thermogravimetric analysis (TGA). Results show that polypyrrole is inserted between bentonite atomic planes. Intercalated bentonite surfaces are covered by conductive polypyrrole particles with uniform size and arrangement, which increases the adsorption capacity of the composite. The adsorption of metal cations (chromium and lead) in aqueous solutions was investigated using PPy-B composites; tests were conducted under various conditions to study the influence of pH, initial concentration, and contact time on the adsorption of these metal cations on the composite PPY-B. The results show that the composites prepared have substantial metal cations adsorption power.
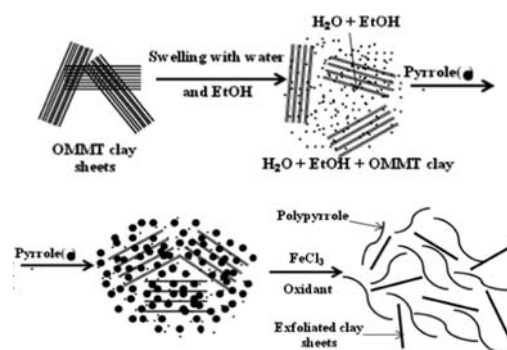
INTRODUCTION

Since the beginning of industrialization, surface and groundwater contamination by heavy metals has been a major problem because of their toxicity towards aquatic life, plants, animals, human beings and the environment.[1] The exponential increase in the presence of heavy metals such as Cr(VI)/(III), Pb(II), Ni(II), Zn(II) Cd(II) and Co(II) in water has raised the concern for lessening the environmental pollution caused by industrial activities and the need for more efficient removal technologies and tougher environmental regulations. Amongst the prevalent heavy metals in aqueous environments, chromium(VI) and lead(II) are known to be very toxic and hazardous elements to living organisms and the environment.

Chromium(VI) can enter the environment through surface waters and even reach groundwater in a number of pathways. These include: discharge of wastewater from industries such as those of electroplating, leather tanning, metal finishing, nuclear power plant, dyeing, photography industries, steel fabrication, plants producing industrial inorganic chemicals, wood treatment units, paints, metal cleaning, fertilizers and textile industries.[2] The acceptable limits of Cr(VI) discharge is 0.05 mg/L in potable water and 0.1 mg/L for surface waters.[2] To comply with the Cr(VI) discharge limits, it is critical that industries treat their effluent streams and decrease this concentration to acceptable levels before release into the natural environment.

---

* Corresponding author:djelnac@yahoo.fr

Lead is a heavy metal with specific toxicity and cumulative effects. The chief sources of lead in water are the effluents of lead and lead processing industries; lead is also used in storage batteries, insecticides, plastic water pipes, food, beverages, ointments and medicinal concoctions for flavoring and sweetening. Lead poisoning in humans causes severe damage to the kidney, nervous system, reproductive system, liver and brain, and causes sickness or death. Severe exposure to lead has been associated with sterility, abortion, stillbirth and neonatal deaths. Children are exposed to lead right from their birth, as children in the embryonic stage receive lead from their mother through the blood. Lead is also known to be toxic to plants, animals and microorganisms. According to the world health organization (WHO), the concentration in a safe drinking water of lead must be below 0.01mg/L.

Recent years have seen large efforts being devoted in developing suitable technologies to effectively remove contaminants such as heavy metals from wastewater. Advances in heavy metals remediation techniques include chemical precipitation, membrane separation, ion exchange, reverse osmosis, solvent extraction and adsorption, amongst others.[3] Apart from adsorption, the aforementioned processes have many disadvantages associated with high energy and reagent requirements, cost, sophisticated equipment and monitoring systems.

Adsorption, however, is a well recognized technique for the treatment of wastewater because of its simplicity, low cost and robustness. Even though activated carbon is the most familiar adsorbent, its widespread use is limited because of factors associated with cost and low capacity for heavy metals.[4] Adsorption techniques though robust in nature, suffers from a massive mass transfer resistance due to the size of conventional adsorbents, which is an important issue. Most of the traditional micro-scale adsorbents have low adsorption capacities and are time consuming to use owing to larger diffusion paths.[5] These drawbacks can be overcome by the application of nano-sized or nanostructured adsorbent materials. Factors such as high surface area, short diffusion route and high extraction efficiencies make nanostructured materials attractive as adsorbents for removal of contaminants from wastewater.[6] Furthermore, adsorption using inexpensive and abundant nanostructured adsorbents would make the removal of heavy metals from wastewater an economically viable alternative technique.

Recently, several researchers have shown interest in clay materials because of their availability, low cost, lamellar structure, chemical and mechanical stability and non toxicity.[7] It is broadly well known that there are three basic species of clay: smectites (such as montmorillonite), kaolinite, and micas; out of which montmorillonite has the highest cation exchange capacity and a good availability in nature.[8]

However, clays have a low surface area owing to some of the inaccessible sites of the stacked lamellar sheets. For this reason, clays have shown to have very low adsorption capacities for heavy metals. This drawback can be overcome through modification by either intercalation or exfoliation of the clay sheets by polypyrrole, with the intention of exposing the inaccessible clay sites for heavy metals adsorption. Amongst the conducting polymers, polypyrrole or PPy is one of the most frequently studied polymers, having high electrical conductivity, ion exchange property, environmental stability, non toxicity, and low cost. Many efforts have been made to synthesize polypyrrole composites for a myriad of applications. For instance, Hong et al.[9] synthesized polypyrrole – montmorillonite composites for application in electronic devices such as light emitting diodes and as a corrosion resistant material, Hosseini et al.[10] studied the effect of polypyrrole–montmorillonite composites powder addition on corrosion performance of epoxy coatings on Al 5000, while Bae et al.[11] synthesized a fully exfoliated nanocomposite from polypyrrole graft copolymer /clay composites for potential applications in many fields such as optics, ionics, electronics, and mechanics . Because of its ion exchange properties, PPy and its modified materials are important adsorbents for removing pollutants from wastewater.[2-5]

Therefore, this work focuses for the first time on the removal of highly toxic Cr(VI) and Pb(II) from wastewater using exfoliated composite via modification of bentonites using a polypyrrole matrix and quantification of the heavy metal adsorption capacity of resulting composites.

EXPERIMENTAL

Materials

The pyrrole monomer was purchased from Sigma-Aldrich, distilled under reduced pressure and kept in a refrigerator before use.

The clay that was used is a white sodium bentonite from the North - West of Algeria. It comes from the Hammam Boughrara (Maghnia) deposit. The bentonite was activated by H_2SO_4 sulfuric acid in order to increase the surface area, porosity and acidity of the surface.

Table 1

Physico-chemical characteristics of bentonite Maghnia

Bentonite	Wpecific surface (m^2/g)	pH	Density	Exchangeable cations (meq /100g)			
				Ca^{2+}	Mg^{2+}	Na$^+$	K$^+$
Maghnia	80	6.2	2.06	30.6	12.8	36.2	9.5

Table 2

Chemical composition (in %) of bentonite

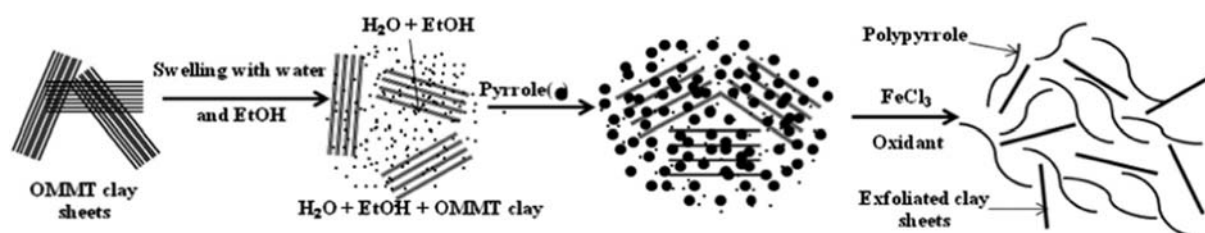| Proportion (%)	SiO$_2$	Al$_2$O$_3$	Fe$_2$O$_3$	CaO	MgO	Na$_2$O	K$_2$O
Bentonite Maghnia	58.61	21.18	2.22	1.23	5.33	1.50	1.05

Fig. 1 – Schematic representation of in situ intercalative polymerization of PPy-B composite.

Activation of bentonite by H$_2$SO$_4$

In a flask for two-necked of 500 ml, equipped with a condenser, stirrer (magnetic stir bar) and a thermometer, 10 mg of dry bentonite and 250 mL of sulfuric acid solution (2N) were introduced, the mixture was then heated to about 100°C for 4 hours using a water bath. The activated bentonite is then filtered and washed with distilled water until no trace of acid remained; it was finally dried at 105° C, then ground and sieved.

Synthesis of the PPy-B composite

The PPy-B composite was synthesized via an in situ chemical oxidative polymerization technique as shown in Fig. 1. In order to get better dispersion, a known weight of bentonite clay (0.5g) was dispersed in water (37.5mL) by stirring the mixture in a conical flask at room temperature. To this, 0.75 mL of pyrrole monomer was injected and the latter mixture was stirred for 2 days for better insertion of the monomer inside the clay sheets. The monomer was then polymerized by adding 7.4g of FeCl$_3$ dissolved in 12.5 mL of distilled water and stirring for 2 hours. To stop the reaction, acetone was added and the resulting black mass was filtered and washed with distilled water until the filtrate were colorless. Finally, the composite was washed with acetone and dried at 95°C under vacuum.

Removal of metal cations by adsorption on PPy-B composite

0.2 g of PPy-B composite was introduced into an erlenmeyer flask containing 50 mL of the test solution. The flask was closed using Parafilm and placed on a stirring plate at room temperature. The contact time was varied from 5 to 180 min. The solid/liquid separation was achieved by gravity filtration. The filtrate obtained was placed in test tubes and analyzed by atomic absorption spectrometry (Thermo Elemental solar energy).

Characterization

Wide-angle X-Ray diffraction (WAXD) patterns were obtained in transmission mode by using a SIEMENS diffractometer equipped with a 2D wiregrid Hi-Star detector, using a Cu-Kα graphite monochromated radiation (λ=0.15418 nm) at 40 kV and 40 mA. WAXD scans were performed at ambient temperature with a 2θ range between 3 and 60°. Samples were inserted in 0.3 mm special glass capillaries.

Fourier-transform infrared spectroscopy (FTIR) measurements were run on a Magna-850 (Thermo Nicolet, Madison, WI) spectrometer using KBr pellets.

Thermogravimetric analysis of the samples were performed using a Mettler Toledo TGA/SDTA 851e apparatus. The heating rate used was 20°C / min, the temperature range between 50 and 850°C under nitrogen and air atmosphere (at a rate of 20 mL / min).

RESULTS AND DISCUSSION

Chromuim and lead adsorption experiments using PPy-B composite

Various tests were conducted to evaluate the adsorption capacity of the composite as a function of various parameters: pH, initial concentration, and contact time.

Effect of pH

The sorption efficiency of Cr(VI) and pb(II) onto PPY-B as a function of pH was investigated by varying the initial pH of the Cr(VI) and Pb(II)

solutions within the range of 2–10; using either NaOH or HCl. The results are presented in Figs. 2 and 3. PH has a significant influence on the adsorption of metal ions, because surface charge, density of the adsorbent and metallic speciation depend on pH.

A gradual decrease in Cr(VI) removal efficiency is observed as the pH increases. To explain this behavior, various mechanisms such as electrostatic attraction / repulsion, chemical interaction and ion ex-change need to be examined, as these may influence adsorption on adsorbent surfaces.[12] According to Cr(VI) speciation, the predominant species of Cr(VI) in aqueous solutions in the pH range 2–6 are monovalent bichromate ($HCrO_4^-$) and divalent dichromate ($Cr_2O_7^{2-}$) ions, while at pH>6 the dominant species is the chromate (CrO_4^{2-}).[2] At low pH, the composite surface becomes positively charged due to the high concentration of hydronium ions (H^+), therefore increasing affinity for the negatively charged $HCrO_4^-$ and $Cr_2O_7^{2-}$ anions to bind on the composite without competing for the adsorption sites. Furthermore, the increased removal efficiency is also due to the anion exchange property of the polypyrrole (PPy) through replacement of the doped Cl^- with either $HCrO_4^-$ or $Cr_2O_7^{2-}$. As the pH increases, more OH^- is present in the solution, thus competing with chromate ions (CrO_4^{2-}) for adsorption active sites and therefore resulting in a low Cr(VI) removal. These results are in agreement with other studies.[13-14] Based on these observations; all subsequent experiments were performed at pH 2.
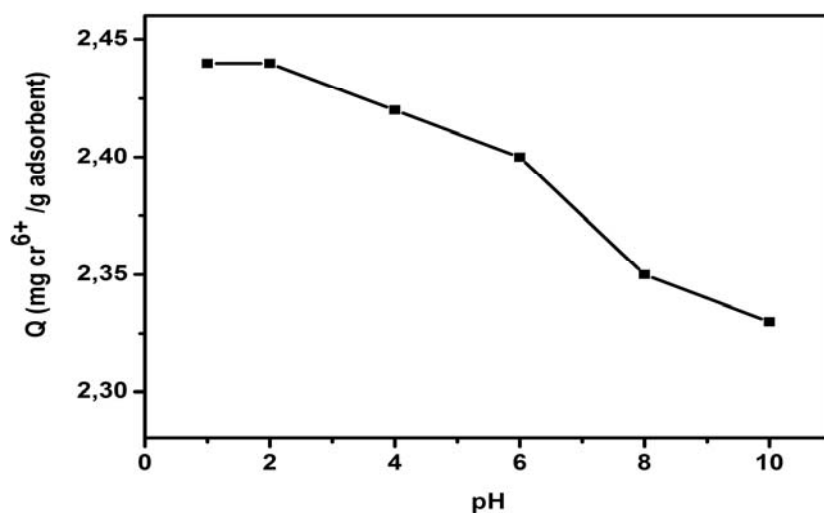

Fig. 2 – Effect of pH on the adsorption of chromium
(Conditions: initial conc. 10mg/L, quantity of composite 4g/L, time 60 min, temp. 23°C, agitator speed 600 rpm).
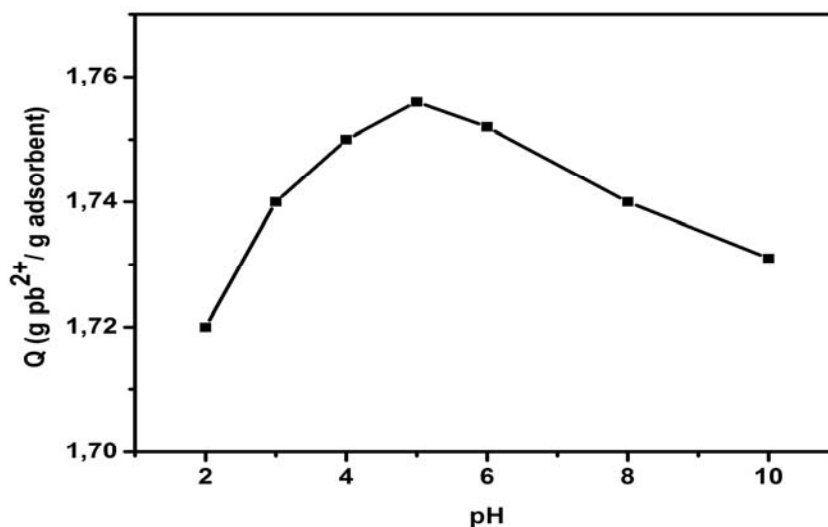

Fig. 3 – Effect of pH on the adsorption of lead
(Conditions: initial conc. 10mg/L, quantity of composite 4g/L, time 60 min, temp. 23°C, agitator speed 600 rpm).

The mechanism of pH dependence on lead(II) ion uptake may be explained by the nature of the composite surface metal binding sites. Fig. 3 shows the effect of pH on the removal of lead(II) ions from an aqueous solution using the PPy-B adsorbent. There is almost no change in the adsorption capacity with increasing pH of the metal solution during the adsorption process up to pH values of 4–6 and the maximum lead(II) ions removal was observed at pH 5. The adsorption of metal ions as a function of initial pH clearly indicated that solution pH played an important role in the adsorption of lead(II) ions by clay based composite. Under highly acidic conditions (pH = 1–2), the adsorption of lead(II) ions is not as effective, since the metal binding sites on the adsorbent are closely associated with H_3O^+ ions which restrict the approach of metal cations as a result of repulsive forces. However, the adsorption increases with increasing solution pH, up to a pH value of 5, since more metal binding sites are exposed to negative charges, attracting positively charged metal ions and adsorbing them onto the composite surface. A decrease in the adsorption of lead(II) ions is observed between pH 5 and pH 10 due to the precipitation of lead hydroxide ions as $Pb(OH)_2$ at higher pH values.[15]

Effect of initial concentration

According to Baral et al.[16] and Devaprasath et al.,[17] adsorption of chromium and lead is greatly influenced by its initial concentration in treated aqueous solutions. Therefore, solutions having initial lead concentration values of 1, 5, 8, 10 and 20 mg/ L were studied and results are shown in Fig. 4.

The adsorption of both metals Cr(VI) and Pb(II) onto the increases with the increase in initial concentration of the metal when the same pH. Time and temperature were used. A similar trend was observed by Bhaumik et al.[18] and Lei et al.[19] The adsoption curves follow a non-linear trend, and reach a plateau at a concentration of 2.5 for Cr(VI) and 1.8 mg/ g for the pb(II). The reduction in the amount of chromium or lead removed after this point is likely due to the increased number of ions in the solution for the same number of sites and the same surface of adsorbent: the composite is reaching its saturation point, and increasing the amount of Cr(VI) and Pb(II) adsorbed per unit mass of the composite then results from metal ions occupying surface sites inaccessible to low concentrations of Cr(VI) and Pb(II). Hence, for further studies, the initial Cr(VI) ion concentration was fixed at 10 mg/L for optimal adsorption.

Effect of contact time

Contact time is an important parameter because this factor can reflect the adsorption kinetics of an adsorbent for a given initial adsorbate concentration. Influence of contact time on adsorption of Cr^{6+} and Pb^{2+} onto PPy-B composite was investigated for the initial metal ion concentration of 10 mg/L for each metal ion and the contact time was varied from 10 to 180 min. Results are shown in Fig. 5.
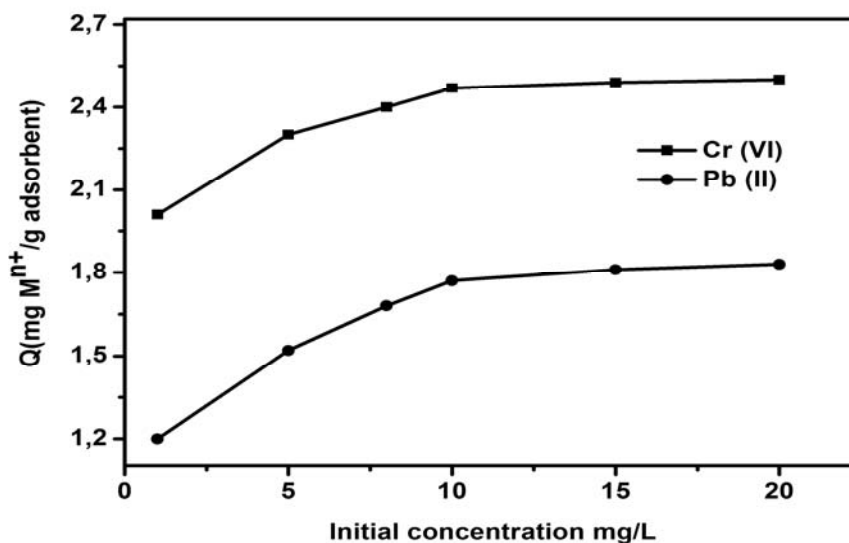

Fig. 4 – The influence of the initial concentration on the adsorption of chromium and lead
(Conditions: quantity of composite 4g/L, pH 5, time 60 min, temp. 23°C, agitator speed 600 rpm).
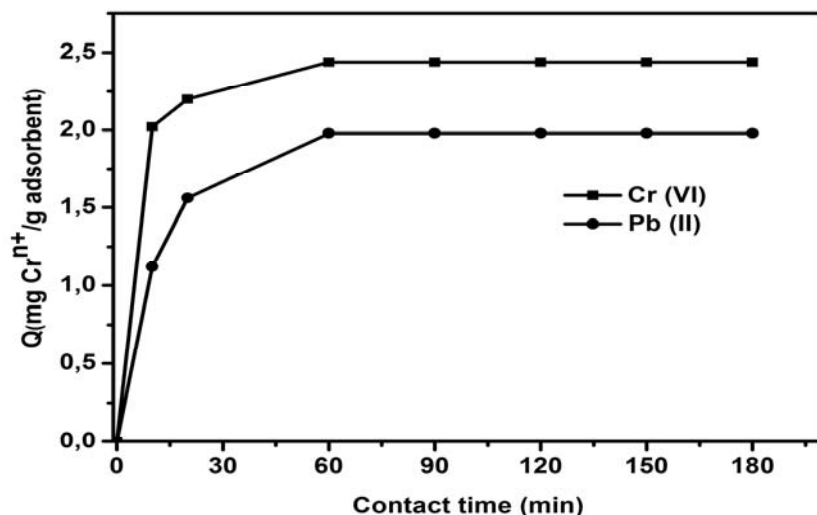
Fig. 5 – The effect of contact time on the adsorption of chromium and lead
(Conditions: initial conc. 10mg/L, quantity of composite 4g/L, pH 5, temp. 23°C, agitator speed 600 rpm).

Characteristic curves of the adsorption kinetics of two metal cations are shown in Fig. 5 above, where we see two stages, the first on for which the adsorption is rapid, while for the second it is slow. This type of two-phase adsorption is also observed in other studies by Dogan et al.[20] and Khraisheh et al.[21] The rapid adsorption step lasts about 35 minutes for each of the two metals and the equilibrium (maximum) adsorption is reached after approximately 60 minutes. The fast initial uptake is due to the availability of abundant active sites for sorption. As these become saturated with time, the step in which a slow rate of adsorption is observed is likely due to composite surface saturation by Cr(VI) or Pb(II) ions, followed by adsorption and desorption processes. These results confirm those previously obtained by Tran Van Son et al.[22] and Argun et al.[23] Therefore, the optimum contact time for the removal of Cr(VI) and Pb(II) ions by PPy-B composite was fixed as 60 min for further adsorption studies.

Adsorption isotherms

Adsorption isotherms are important for research into an adsorption process. Numerous isotherm equations have been reported, and two major isotherms, the Freundlich and Langmuir isotherms, were applied to establish the relationship between the amount of Cr^{6+} and pb^{2+} ions adsorbed by the composite and the equilibrium concentration in aqueous solution.

Langmuir isotherm

This isotherm assumes that metal uptake occurs on a homogenous surface by monolayer adsorption without interactions between the active sites on the adsorbent or adsorbed metal ions.[24] The linearized form of the Langmuir isotherm is given in eq. (1).

$$Ce/qe = Ce/qm + 1/qmb \qquad (1)$$

where Ce (mg/l) is the concentration of the metal ion (lead or chromium) in equilibrium, qe (mg/g) is the equilibrium uptake capacity, qm (mg/g) is the maximum adsorption capacity corresponding to a complete monolayer coverage and b (L/mg) is the Langmuir isotherm constant which quantitatively reflects the affinity between the adsorbent and the adsorbate. A linear plot of Ce/qe against Ce confirms the isotherm and is shown in Fig. 6. The constants qm and b were calculated from the slope and intercept respectively. The Langmuir isotherm parameters are given in Table 3.

Freundlich isotherm

The Freundlich isotherm unlike the Langmuir isotherm assumes that adsorption takes place on a heterogeneous surface which involves a multilayer adsorption of metal ions.[25] The linear form of the Freundlich equation is given in eq. (2).

$$lnqe = lnKf + [1/n]lnCe \qquad (2)$$

where n is a dimensionless constant describing the adsorption intensity and Kf (L/g) is the Freundlich isotherm constant describing the adsorption capacity of the adsorbent. This isotherm was confirmed by the plot of lnqe against lnCe shown in Fig. 7. The constants n and Kf were respectively obtained from the slope and intercept. The

Freundlich isotherm parameters are presented in Table 3. A value of n above unity indicates a favourable adsorption. Again a favourable adsorption was obtained between lead(II) or chromium(VI) ions, and PPy-B composite.

The results obtained for the two isotherms confirm the affinity of the adsorbent PPy-B towards the two metal cations, with chromium better adsorbed than lead. Indeed, the highest value

of k and the smallest value of n are observed for Cr(VI) ions.

The correlation coefficient values (R) are higher for the Langmuir isotherm than for the Freundlich isotherm, which indicates that the Langmuir isotherm equation represents better the adsorption of Cr(VI) and Pb(II) by the composite. This is probably due to the uniform distribution of the assets at the composite surface sites.
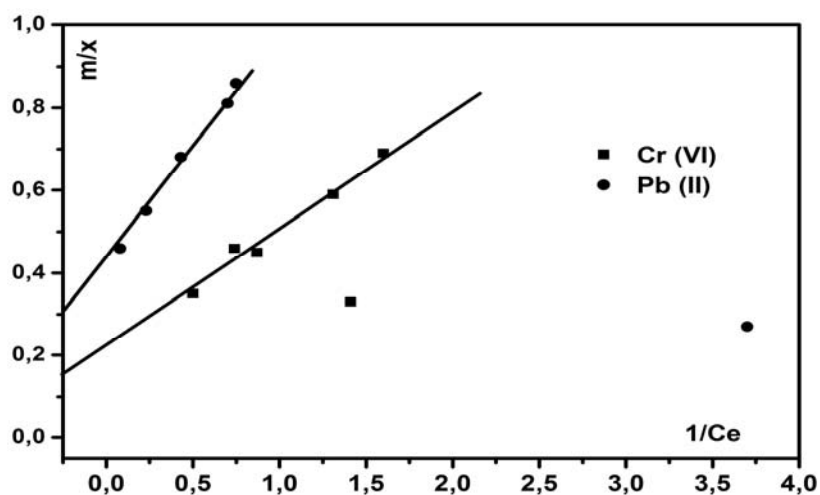
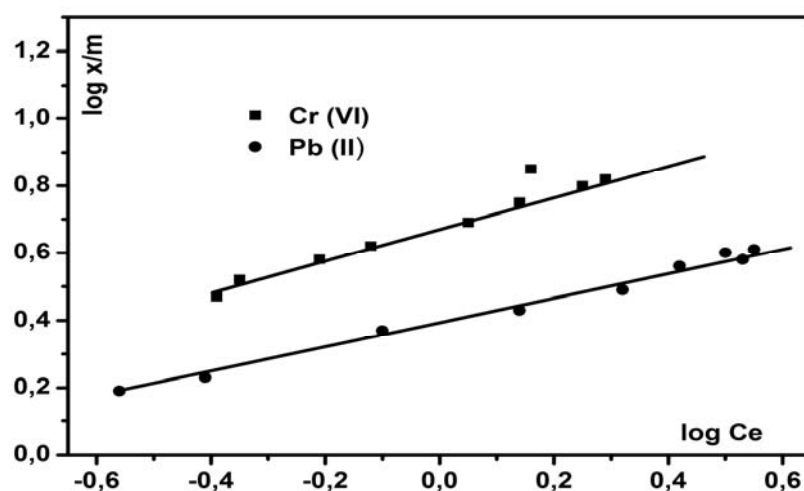

Fig. 6 – Langmuir adsorption isotherm.

Fig. 7 – Freundlich adsorption isotherm.

Table 3

Constants for Langmuir and Freundlich isotherms for chromium and lead

Adsorbent PPy-B	Langmuir isotherm			Freundlich isotherm		
	q_e	b	R%	K	n	R%
Cr(VI)	7.14	5.55	99.86	6.12	2.08	96
Pb(II)	5.26	4	99.25	3.32	2.27	98.25

Characterization of bentonite,
PPy and PPy-B composite

The spacing between clay platelets, or gallery spacing, is an indicator of the extent of intercalation/ exfoliation of clay platelets within a polymer matrix and can be observed by using WAXD analysis.

Peak positions and d-spacings are reported in Table 4, along with an indexation proposed by comparison to the literature.[26-28]

Generally, narrow intense reflections in the 3°- 9° (2θ) range indicate an ordered intercalated composite.[29] The reflection observed in this region for montmorillonite is indexed as the (001) diffraction plane, and corresponds to the interlayer distance. In completely exfoliated composites, on the other hand, single silicate layers are homogeneously dispersed in the polymer matrix, and the XRD patterns show no distinct diffraction peak in the range, this range according to Zhu *et al.*[30] Changes in peak position towards smaller values indicate that intercalated material has been inserted, thus increasing the interlayer distance.

Fig. 8 shows the XRD powder patterns of PPy, bentonite, and PPy-B composite. The XRD pattern of the initial PPy exhibits a broad peak which is centered at around 26°, typical of amorphous polymers. On the other hand, the XRD patterns of bentonite and PPy-B composite both display a sharp diffraction peak in the 3°- 9° region, and its position has shifted from 7.60 ° in the initial bentonite to 7.40º in the PPy-bentonite composite. This shift indicates that larger interplaner distances now exist (the d spacing having increased from 13.4 to 15.5 Å), which suggests that some PPy has intercalated and flocculated the silicate layers of clay. The intercalation driving force of cationic polypyrrole macromolecules into the bentonite interlayer zone is attributed to adsorption to hydrated sodium ions and to the formation of hydrogen-bonding interactions between N-H groups of polypyrrole and surface oxygen atoms of bentonite. Previous work in the literature shows is in agreement with that the present work, and shows that conducting PPy intercalates between the clay layers.[31]
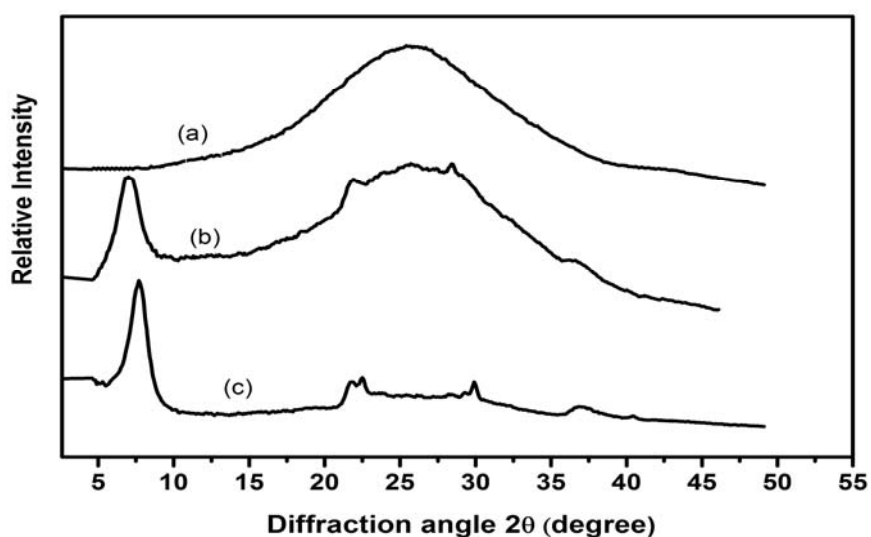

Fig. 8 – XRD powder diffraction diagram of PPy (a), PPy-B composite (b) and bentonite (c).

Table 4

D-Spacings for Bentonite and PPy-B

Bentonite		PPy-B		Phase and Miller indices of the reflection
2θ (°)	d (Å)	2θ (°)	d (Å)	
7.6	13.4	7.4	15.5	Montmorillonite (100)
22.10	4.02	22.10	4.02	Quartz (402)
29.97	2.99	28.3	3.19	Montmorillonite (005)
36.55	2.45	36.55	2.45	Quartz (117)
40.34	2.23	40.34	2.23	Quartz (111)

FTIR spectra provide additional information about the structure of PPy-B composites studied. Representative spectra are shown in Fig. 9.

Examination of our results and those of the literature[32-34] shows absorption bands presented in the following table.

The bentonite clay material has characteristic peaks at 3626 cm^{-1}, 3440 cm^{-1}, 1634 cm^{-1}, 1041 cm^{-1}, 913 cm^{-1} and 470 cm^{-1}. The peaks at 3626 cm^{-1}, 3440 cm^{-1} and 1641 cm^{-1} are due to absorbed water, the peaks at 1041 cm^{-1} is attributed to Si-O bonds, the band around 913 cm^{-1} to Al-OH groups, and the band at 470 cm^{-1} to Mg-OH bonds. The PPy chain absorption bands have been attributed previously in the literature.[35, 36] A strong broad band at around 3434 cm^{-1} corresponds to the N-H stretching vibration for PPy macromolecules. The PPy-B composites spectra clearly exhibits characteristic absorption peaks associated with both PPy chains and bentonite. Small shifts in absorption maximum and alteration of band shape are results of changes in the nearest surrounding functional groups. These observations are illustrated in Fig. 9 for bands in region 1000–1700 cm^{-1} For example, the 1454 cm^{-1} band of pure PPy shifts to 1442 cm^{-1} for the PPy-B composite and the 3434 cm^{-1} PPy band shifts to 3440 in PPy-B. Thus, FTIR spectroscopy also supplies evidence of possible interactions between PPy bentonite clay.
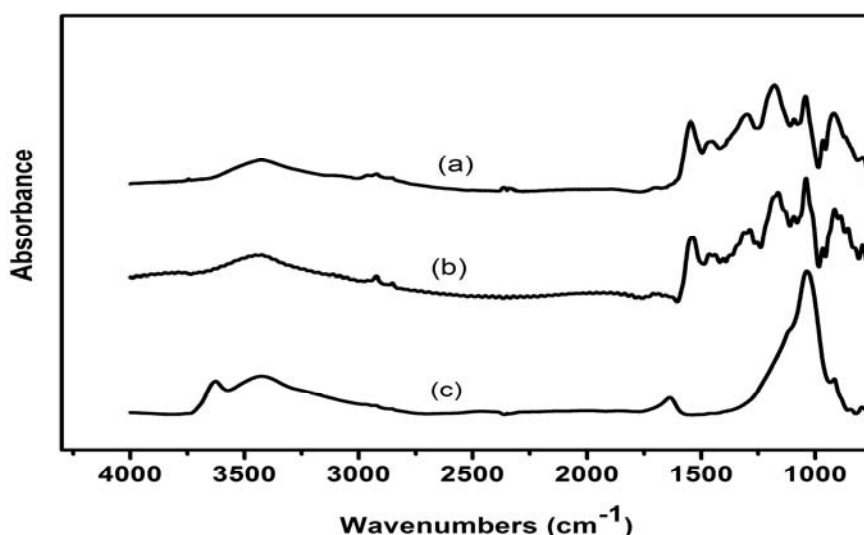

Fig. 9 – FTIR spectra of PPy (a), PPy-B composite (b) and bentonite (c).

Table 5

FTIR band attributions for bentonite, PPy and PPy-B

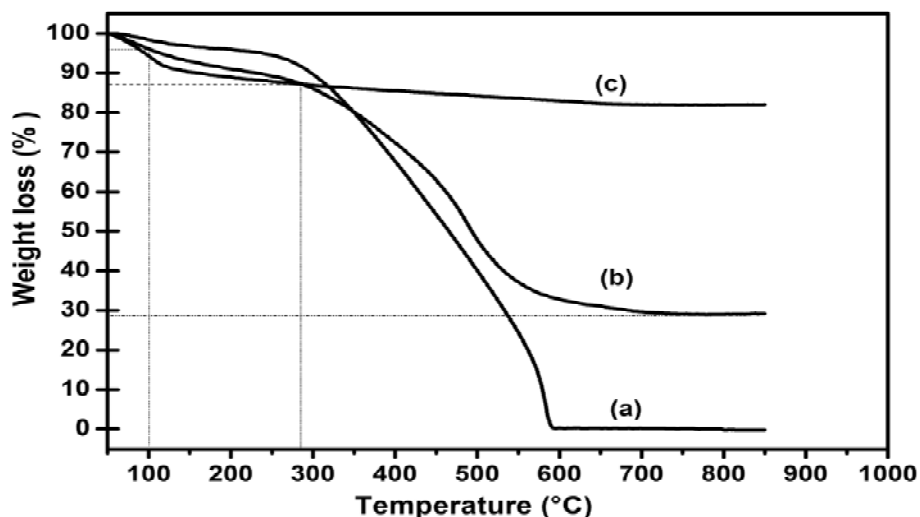| Sample	v (cm^{-1})	Attribution
Bentonite	3626	ν O-H
	3440	δ H-O-H
	1634	ν H-O-H
	1041	ν Si-O-Si
	913	δ Al-OH
	470	δ Mg-OH
PPy	3434	ν N-H
	1554	ν C=C C-C, pyrrole ring
	1468	ν C-N
	1294	δ $_{in-plane}$ C-H, aromatic groups
	1189	δ $_{in-plane}$ C-H, aromatic disubstituted groups
PPy-B	3440	ν N-H
	1542	ν C=C aromatic groups
	1468	ν C-N of PPy
	1041	ν Si-O-Si
	1294	δ C-H aromatic PPy groups
	1189	δ C-H aromatic di-substited PPy groups

Fig. 10 – TGA of PPy (a), PPy-B composite (b) and bentonite (c).

Table 6

text

| | Mass loss (%) | | | | (%) Of polymer intercalated |
Sample	T< 100°C	T : 100- 300°C	T: 300-700°C	T : 700-850°C	
Bentonite	6	7	5	0	-
PPy	0.9	8	91	0	-
PPy-B	4	9	58	0	58%

Thermal stability was investigated using TGA under a nitrogen atmosphere. Fig. 10 shows TGA thermograms of of PPy, PPy-B composite and bentonite. As expected, the PPy-bentonite composites combine both features. In the 600-800 ºC region, the polymer has finished degrading, but bentonite is still intact, apart from a small loss of water near 100 ºC, which allows to use TGA to determine the quantity of polymer created by the polymerisation reaction.

Table 6 reports relative weight loss of bentonite, PPy and PPy-B in different regions of the scan, along with the percentage of polymer intercalated into bentonite.

The first weight losses below 100°C is attributed to water release, which is mainly observed for bentonite, but which is also present in the polymer, and is attributed water adsorption, as the samples have been dried only under desiccant to limit thermal degradation prior to measurements. For bentonite, a weight loss of 7% occurs in the temperature range, and a further 5% loss between 300 and 700 °C is also observed. These losses are due from the water content of the structure of bentonite (OH octahedral layers).[37] Between 290 and 600 ºC, gradual weight losses are observed for pure PPy and for the PPy-B composite. The total mass loss up to 850 °C can be

estimated to be about 5%, 91% and 58% for bentonite, PPy and PPy-B composites respectively. The in situ intercalative polymerized PPy-B composite shows better thermal stability than other PPy-clay composites reported by other groups,[38,39] but consistent with data from other groups.[2] In the present study, the PPy-B composite degradation curve is similar to that of PPy; degradation of PPy-B is mainly controlled by PPy. Observed weight losses suggest that the thermal stability of the PPy-B composites is enhanced because of the barrier effect of the clay layer structure and by the interactions between PPy and bentonite. Interfacial interactions between the intercalated nanolayer of positively charged polymer backbone and the negatively charged clay layer surface are a key factor for enhancing thermal stability. Accordingly, the clay platelets have a shielding effect and slow down the decomposition rate of the composite.

CONCLUSIONS

In this study, the chemical polymerization of pyrrole was performed in the presence of bentonite in order to prepare PPY–B composites. Adsorption of aqueous metal ion s (chromium and lead) solutions was first investigated. Adsorption tests

were conducted under various conditions to study the influence of the main parameters (pH, initial concentration, and contact time). The results showed a good adsorption capacity of heavy metals for the studied composite. The best results for removal of heavy metals were obtained at pH = 6, initial concentration = 10 mg/L, contact times of 60 minutes and a temperature of 23 ° C.

The PPy-bentonite composites were then investigated by X-ray diffraction and FTIR spectrsocpoy. Change in the (100) bentonite peak position clearly indicates an increase in interplanar spacing, in agreement with PPy intercalation into the layers of bentonite. FTIR peak position shifts further confirmed that interactions occur between polypyrole and bentonite layers. Intercalation of PPY is therefore proposed as being responsible for the observed increase in adsorption capacity of the composite as compared to the initial bentonite.

The application of linearized forms of Freundlich and Langmuir laws allowed to verify that these two models were applicable, and confirms that chrome is better secured than lead, with maximum capacities q_m of 7.14 mg/g and 5.26 mg/g respectively for chromium and lead. A significantly higher K intercept value is also observed for chromium(Cr^{6+}), which confirms the strongest PPy-B affinity for this ion.

REFERENCES

1. Y. F. Shen, J. T. ang, Z. H. Nie, Y. D.Wang, Y. Ren and L. Zuo, *Bioresour. Technol.*, **2009**, *100*, 4139-4146.
2. M. Bhaumik, A. Maity, V. V. Srinivasu and M. S. Onyango, *J. Hazard. Mater.*, **2011**, *190*, 381-390.
3. M. Khamis, F. Jumean and N. Abdo, *J. Hazard. Mater.*, **2009**, *160*, 948-952.
4. Y. Li, B. Gao, T. Wu, D. Sun, X. Li, B. Wang and F. Lu, *Water Res.*, **2009**, *43*, 3067-3075.
5. M. Bhaumik,T. Y. Leswifi, A. Maity,V. V. Srinivasu and M. S. Onyango, *J. Hazard. Mater.*, **2011**, *186*, 150-159.
6. K. Ghanemi, Y. Nikpour, O. Omidvar and A. Maryamabadi, *Talanta*, **2011**, *85*, 763-769.
7. K. G. Bhattacharya and S. S. Gupta, *Adv. Colloid Interface Sci.*, **2008**, *140*, 114-131.
8. S. Babel and T. A. Kurniawan, *J. Hazard. Mater.*, **2003**, *B97*, 219-243.
9. S. H. Hong, B. H. Kim, J. Joo, J. W. Kim and H. J. Choi, *Curr. Appl. Phys.*, **2001**, *1*, 447-450.
10. M. G. Hosseini, M. Raghibi-Boroujeni, I. Ahadzadeh, R. Najjar and M. S. Seyed Dorraji, *Prog. Org. Coat*, **2009**, *66*, 321-327.
11. W. J. Bae, K. H. Kim, W. H. Jo and Y. H. Park, *Polym.*, **2005**, *46*, 10085-10091.
12. S. K. Srivastava, A. K. Singk and S. Ashutosh , *Environ. Technol.*, **1994**, *15*, 353-360.
13. M. Sanchez-Polo and J. Rivera-Ultrilla, *Environ. Sci. Technol.*, **2002**, *36*, 3850-3854.
14. F. Brito , J. Ascno and S. Mateo, *Polyhedron*, **1997**, *16*, 3835-3846.
15. G. M. Gadd and H. J. Rehm (Ed.), "Biotechnology", VCH, Weinheim, 1988, p. 401-433.
16. S. S. Baral, S. N. Das, G. R Chandhury and P. Rath, *Adsorption*, **2008**, *14*, 111-121.
17. P. M. Devaprasath, J. S. Solomon, B.V. Thomas, *J. Appl. Sci. Environ.*, **2007**, *2*, 77-83.
18. M. Bhaumik, A. Maity, V. V. Srinivasu and M. S. Onyango, *Chem. Eng. J.*, **2012,** *181-182*, 323-333.
19. Y. Lei, X. Qian, J. Shen and X. An, *Ind. Eng. Chem. Res.*, **2012**, *51*, 10408-10415.
20. M. Dogan, M. Alkan, A. Turkyilmaz and Y. Ozdemir, *J. Hazard. Mater.*, **2004**, *109*, 141-148.
21. M. A. Khraisheh, Y. S. AL-Degs, S. J Allen and N. M. Ahmed, *Ind. Eng. Chem. Res.*, **2002**, *41*, 1651-1657.
22. S. Tran Van and Q. Tran Van, *J. Sci, Earth. Sci.*, **2012**, *28*, 37-43.
23. M. E. Argun, S. Dursun, C. Ozdemir and M. Karatas, *J. Hazard. Mater.*, **2007**, *141*, 77-85.
24. I. Langmuir, *J. Am. Chem. Soc*, **1918**, *40*, 1361-1368.
25. K. Vijayarahgavan, J. R. Jegan, K. Palanivelu and M. Velan, *Adsorption. Sci. Technol.*, **2005**, *23*, 303-311.
26. J.H.Yeum and M.R. Karim, *J. Polym. Sci. B,* **2008**, *46*, 2279-2285.
27. C. Meltem and O. Müserref, *J. Therm. Compos. Mater.*, **2011**, *25*, 505-520.
28. J. W. Kim, F. Liu, H. J. Choi, S.H. Hong and J. Joo, *Polym.* **2003**, *44*, 289-293.
29. A. B. Morgan and J. W. Gilman, *J. Appl. Polym. Sci.*, **2003**, *87*, 1329-1338.
30. J. Zhu, X. Wang, F. Tao, G. Xue, T. Chen, P. Sun, Q. Jin and D. Ding, *Polym.*, **2007**, *48*, 7590-7597.
31. J. W. Kim, F. Liu and H. J. Choi, *J. Ind. Eng. Chem.*, **2002**, *8*, 399-403.
32. J. M. Yeh, C. P. Chin and S. Chang, *J. Appl. Polym. Sci.*, **2003**, *88*, 3264-3272.
33. T. Z. Rizvi and A. Shakor, *J. Phys. D. Appl. Phys.*, **2009**, *42*, 1-6.
34. S. V. Kasisomayajula, X. Qi, C. Vetter, K. Croes, D. Pavlacky and V. J. Gelling, *J. Coat. Technol. Res.,* **2010**, *7*, 145-158.
35. J. M. Yeh, C. P. Chin and S. Chang, *J. Appl. Polym. Sci.*, **2003**, *88*, 3264-3272.
36. J. Liu and M. Wan, *J. Mater. Chem.*, **2001**, *11*, 404-407.
37. T. Wang, W. Liu, J. Tian, X. Shao and D. Sun, *Polym. Compos.*, **2004**, *25*, 111-117.
38. Y. C. Liu and M. D. Ger, *Chem. Phys. Lett.,* **2002**, *962*, 491-496.
39. S. J. Peighambardoust and B. Pourabbas, *Macromol. Symp.*, **2007**, *247*, 99-109.